

Heterophase Polymerization of Different Methacrylates: Effect of Alkyl Ester Group on Kinetics and Colloidal Behavior

Víctor M. Ovando-Medina,¹ Miguel A. Corona-Rivera,¹ Alfredo Márquez-Herrera,²
Tania E. Lara-Ceniceros,³ Ricardo Manríquez-González,⁴ René D. Peralta⁵

¹Ingeniería Química, COARA—Universidad Autónoma de San Luis Potosí, Matehuala San Luis Potosí 78700, México

²Ingeniería Mecánica Administrativa, COARA—Universidad Autónoma de San Luis Potosí, Matehuala San Luis Potosí 78700, México

³Centro de Investigación en Materiales Avanzados, Alianza Norte 202, Parque de Investigación e Innovación Tecnológica, Apodaca Nuevo León 66600, México

⁴Departamento de Madera, Celulosa y Papel, CUCEI, Universidad de Guadalajara, Jalisco 45020, México

⁵Centro de Investigación en Química Aplicada, Saltillo Coahuila 25100, México

Correspondence to: V. M. Ovando-Medina (E-mail: ovandomedina@yahoo.com.mx)

ABSTRACT: In this article, methyl- (MMA), ethyl- (EMA), *n*-butyl- (BMA), *n*-hexyl (HMA), and 2-ethyl hexyl (2-EHMA) methacrylates were homopolymerized in heterophase at 60°C using sodium dodecyl sulfate as surfactant and potassium persulfate as initiator. The effects of monomer content in the reaction mixture (2.5 and 3.5 wt %) and the alkyl ester groups of the methacrylates on the kinetics, average particle diameter (D_p), molar masses, tacticity, and glass transition temperature (T_g) were studied. The final weight average molecular weights were in the range of 4.53×10^5 to 2.78×10^6 g/mol with polydispersities between 1.7 and 3.1 for different methacrylates. For 2.5 wt % of monomer concentration, the order of increase in polymerization rate was $R_{p_{HMA}} > R_{p_{BMA}} > R_{p_{2-EHMA}} > R_{p_{EMA}} > R_{p_{MMA}}$, whereas for 3.5 wt % of monomer concentration was $R_{p_{BMA}} > R_{p_{HMA}} > R_{p_{2-EHMA}} > R_{p_{EMA}} > R_{p_{MMA}}$. This behavior was ascribed to the differences in the water solubility, monomer partitioning between the different phases, and monomers reactivity. The D_p values varied between 42 and 65 nm, increasing according to the hydrophobicity of each monomer. ¹³C-NMR (nuclear magnetic resonance) and differential scanning calorimetry analysis demonstrated that 79–87% of syndiotactic configuration was obtained for the different polymers. The steric effect of the alkyl ester length in the methacrylates contributed directly to promote the syndiotactic configuration. Nevertheless, T_g values (between -7 and 120°C) for these polymers decreased when the alkyl ester length increased. © 2013 Wiley Periodicals, Inc. *J. Appl. Polym. Sci.* **2014**, *131*, 40191.

KEYWORDS: stereochemistry; tacticity; latices; radical polymerization; surfactants; DSC

Received 17 April 2013; accepted 14 November 2013

DOI: 10.1002/app.40191

INTRODUCTION

Heterophase polymerization is a generic term applied to methods that produce polymeric lattices,¹ where the monomer(s) and products (polymers) are insoluble in the reaction medium. The processes in this category are emulsion, miniemulsion, and microemulsion polymerizations, and their variations that include the continuous addition of reagents to the polymerization system. Common features of these processes are the following: (1) at least two phases are present; (2) the system has spatial density differences; (3) transport of monomer occurs between the phases; and (4) the reaction occurs under nonequilibrium conditions. Advantages of reactions carried out in heterophase systems are the easiness of removal of the heat of reaction, the low viscosity (independent of

the polymer molecular weight) of the reaction system at all times and the possibility to feed monomer or an emulsion during the reaction, monomer concentration at the polymerization loci can be maintained stationary at its highest level so that the rate of reaction can be kept high during the whole polymerization, and the particle size distribution (PSD) and average particle diameter (D_p) can be tailored over wide ranges.²

Although heterophase polymerization of some alkyl methacrylates has been studied separately,^{3,4} there are no reports addressed to find a correlation between the effect of the alkyl group structure (length and volume) with the kinetic and colloidal behavior. For example, Morgan et al.³ and Kaler et al.^{5,6} proposed a very simple mathematical model to make a kinetics

Additional Supporting Information may be found in the online version of this article.

© 2013 Wiley Periodicals, Inc.

study about microemulsion polymerization of *n*-hexyl methacrylate (HMA). Their model predicts the conversion and polymerization rate through reaction for HMA very well. However, contrary to the experimentally observed, their model indicates that the maximum polymerization rate always occurs at conversions of 39%, independently of the type of monomer polymerized. Katime et al.⁷ studied the effect of monomer, initiator concentrations, as well as the temperature in the polymerization of HMA in three-component microemulsions stabilized with dodecyltrimethylammonium bromide (DTAB). The final latexes obtained were bluish, transparent, and translucent. Particle sizes and molar masses were on the order of 20 nm and 3×10^6 g/mol, respectively. In all the cases, high reaction rates and final conversions near to 98% were observed. In fact, they found that temperature has a strong effect on reaction rate and conversion. Polymerization kinetics in microemulsions of *n*-butyl methacrylate (BMA), tert-butyl methacrylate, HMA, and styrene prepared with DTAB were studied by Kaler et al.^{8,9} They modified their previous mathematical model in order to examine the effect of monomer partitioning on the kinetics of polymerization. In both the cases (experiment and theory), the results suggested that monomer partitioning during microemulsion polymerization strongly depends on the microemulsion composition, especially on the distance to the phase boundary. Thus, the values of conversion at which the maximum polymerization rate occurred were well predicted with this model.

Microemulsion polymerization of methacrylate monomers has been reported as a manner to control tacticity in polymers. Tang et al.⁴ studied the effect of alkyl side group of some methacrylates as methyl methacrylate (MMA), ethyl methacrylate (EMA), cyclohexyl methacrylate (CHMA), iso-butyl methacrylate (iBMA), and benzyl methacrylate (BzMA) on the polymer tacticity configuration through a modified microemulsion polymerization procedure (seeded semicontinuous polymerization). They found that the syndiotacticity of the product decreased when the polymerization was carried out at a temperature far above the T_g of the resulting polymer. Furthermore, tacticity of the polymer was affected by the monomer structure: a monomer with a bulkier alkyl side group would promote the formation of a polymer with high syndiotactic configuration. Conversely, Mendizábal et al.¹⁰ studied the polymerization of MMA in three-component microemulsions using different surfactants [DTAB, DTAC, sodium dodecyl sulfate (SDS), and bis(2-ethylhexyl) sulfosuccinate sodium (AOT)]. Stable latices of poly(methyl methacrylate) (PMMA) with particle sizes below 46 nm and polymer with high molecular weights (1×10^6 g/mol) were obtained. ¹H- and ¹³C-NMR (nuclear magnetic resonance) spectra of these PMMAs indicated the presence of polymers with between 72 and 78% syndiotactic configuration. Such values of syndiotacticity are larger than those reported for commercial PMMA. The authors interpreted these results on the basis that due to the small size of the particles (18–45 nm), chains growth takes place in a confined space that can accommodate better the syndiotactic configuration. Also, as a result of the high syndiotactic configuration, the T_g was higher than the previously reported value in the literature.

The aim of this article was to report a systematic study of the effect of the structure of alkyl ester groups of MMA, EMA, BMA, HMA, and 2-ethyl hexyl methacrylate (2-EHMA) during heterophase polymerization to elucidate their influence on the kinetics, molar masses, particle diameters, tacticity, and glass transition temperatures (T_g) of the corresponding homopolymers.

EXPERIMENTAL

Polymerizations

All monomers (Aldrich, >98%), were purified by distillation under reduced pressure. The surfactant SDS (Hycel, Guadalajara, Mex. >99%) and the initiator potassium persulfate (KPS) (Aldrich, >98%) were used as received. The water used in the experiments was bidistilled grade. Argon (InfraTM of ultra-high purity) was used to remove oxygen from the system. Kinetic behaviors were determined by dilatometry as follows: water (36.7 or 36.5 g for 2.5 or 3.5% of monomer concentrations, respectively), surfactant (2.35 or 2.32 g for 2.5 or 3.5% of monomer concentrations, respectively), and monomer (1.01 or 1.41 g for 2.5 or 3.5% of monomer concentrations, respectively) were placed in a vial and homogenized. After that, 35 g of mixture was charged to a dilatometer (a reactor of 35 mL with a capillary of 40 cm height and 1 mm inner diameter, and a port with a septum at the bottom). A syringe was used to fill the dilatometer injecting the mixture of water, surfactant, and monomer to reach 4 cm of capillary height. The dilatometer was immersed into a water bath of glass walls in order to observe capillary height changes at 60°C through 10 min noting an increase of capillary height of approximately 25 cm; then, the dilatometer was placed into an ice bath to eliminate bubbles. This procedure was repeated until no bubble formation was observed. Initiator (1 wt % respect to monomer) was dissolved in 0.5 mL of water and injected to reaction mixture. The dilatometer was heated to reaction temperature and the capillary height reached between 25 and 35 cm. Polymerizations started after 10 min and the capillary height decreased. Height data were registered every 5 s. Conversions were calculated using eq. (1):

$$x = \frac{\pi d^2}{4} (h_0 - h_t) \times \left(\frac{1}{\frac{w_0(\rho_P - \rho_M)}{\rho_M \rho_P}} \right) = \frac{\Delta V}{V_0 k} \quad (1)$$

where d is the capillary inner diameter in cm; h_0 and h_t are the capillary heights in cm at time zero (reaction time from the start of the polymerization, i.e., from the start of the decrease in capillary height) and at a given time, respectively; w_0 represents the initial grams of monomer; ρ_P and ρ_M are the polymer and monomer densities, respectively. Density values used in eq. (1) were: $\rho_{\text{PMMA}} = 0.94$ g/cm³, $\rho_{\text{EMA}} = 0.9158$ g/cm³, $\rho_{\text{BMA}} = 0.895$ g/cm³, $\rho_{\text{HMA}} = 0.863$ g/cm³, and $\rho_{\text{2-EHMA}} = 0.885$ g/cm³, respectively; whereas for the corresponding homopolymers were $\rho_{\text{PMMA}} = 1.18$ g/cm³, $\rho_{\text{PEMA}} = 1.119$ g/cm³, $\rho_{\text{PBMA}} = 1.053$ g/cm³, $\rho_{\text{PHMA}} = 1.007$ g/cm³, and $\rho_{\text{P2-EHMA}} = 0.979$ g/cm³, respectively.

In eq. (1), ΔV is the change in the volume of capillary, V_0 is the initial volume and k is known as the contraction factor given by $(\rho_P - \rho_M) / \rho_P$. Equation (1) can be also expressed as follows:

$$x = \frac{\Delta h}{h_0 - h_\infty} = \frac{h_0 - h_t}{h_0 - h_\infty} \quad (2)$$

where h_∞ is the capillary height at full conversion ($t \rightarrow \infty$). In this article, we used eq. (2) in the calculation of conversions by dilatometry.

In order to obtain enough polymer and samples of latices to determine final properties, batch polymerizations were carried out using a spherical glass-jacketed reactor (250 mL) with two inlets and one port at the bottom for sampling. Magnetic stirring (cylindrical stirring bar of 1 in. \times 1/4 in. and 200 rpm) was used in all reactions. A condenser with reflux was mounted in one neck of the reactor. Water (137.5 or 136.1 g for 2.5 or 3.5% of monomer concentration, respectively), SDS (8.8 or 8.7 g for 2.5 or 3.5% of monomer concentration, respectively), and monomer (3.75 or 5.25 g for 2.5 or 3.5% of monomer concentration, respectively) were charged to the reactor and bubbled with argon for 1 h. After this period, the temperature was raised to 60°C by passing water from a bath through the jacket of the reactor. To start polymerizations, KPS (1% respect to monomer) dissolved in 2 mL of water was added in one shot using a syringe. Samples were taken at different times and dried at 60°C in an oven during 48 h to determine conversions by gravimetry from mass balances.

Characterization

PSD and D_p were determined at 25°C by Dynamic Light Scattering (Nano S-90, Malvern) at an angle of 90°. Intensity correlation data were analyzed by the method of cumulants to provide the average decay rate, $\langle \Gamma \rangle (=q^2D)$, where q is the scattering vector and D is the diffusion coefficient. The measured diffusion coefficients were represented in terms of apparent radii by using Stokes law and assuming the solvent has the viscosity of latex.¹¹ Dried polymer samples were washed with hot water in order to remove the remaining initiator and surfactant. The washed samples were dried for 48 h at 60°C and analyzed by gel permeation chromatography (GPC). All samples were dissolved in tetrahydrofuran (Aldrich, HPLC-grade). A GPC Hewlett-Packard HP series 1100 apparatus equipped with a refractive index detector and three PL Gel serial columns (pore sizes 10³, 10⁵, and 10⁶ Å) was used to determine molecular weight distributions. The molecular weights were determined on the basis of a calibration curve constructed with narrow polystyrene standards. Glass transition temperatures of the homopolymers were determined by differential scanning calorimetry (DSC) (TA Instruments DSC Q200) using aluminium pans (Tzero®) with nitrogen flux at 100 mL/min. Temperature scans were made between 10 and 200°C for homopolymers of MMA, EMA, and BMA and from -30 to 60°C for the homopolymers of HMA and 2-EHMA. A heating rate of 10°C/min was used in the DSC analysis.

The tacticity of final polymers in terms of triads was determined by ¹³C-NMR (Varian Gemini 2000 Spectrometer, 200 MHz). Washed and dried samples of polymers were dissolved in deuterated chloroform (CDCl₃) and analyzed at carbon frequency of 50.28 MHz. Tacticity was determined by integration of spectra signals corresponding to carbonyl groups and the quaternary carbon. From the RMN spectrum it was possible to

evaluate the type of each stereochemical configuration: [syndiotactic (rr), heterotactic (rm), and isotactic (mm)] of the final polymers. Calculation of syndiotacticity percentage (RR) in each polymer was calculated using the following eq. (3):

$$RR = \frac{A_{(rr)} + \frac{1}{2}A_{(rm)}}{A_T} \times 100 \quad (3)$$

where $A_{(rr)}$ and $A_{(rm)}$ represent the values of integrated area of the signals corresponding to syndiotactic and heterotactic configurations, respectively. A_T is the sum of all areas that comprise the tacticity of the polymer in each region of spectra [$A_{(rr)} + A_{(rm)} + A_{(mm)}$].¹²

RESULTS AND DISCUSSION

It was observed in the dilatometer that at 60°C MMA and EMA formed microemulsions before the initiator was injected. On one hand, BMA, HMA, and 2-EHMA formed emulsions very near to the limit of single phase microemulsions and, upon polymerization, the reaction mixture turned bluish and translucent as with MMA and EMA monomers. On the other hand, it was observed that experimental conversion data determined by dilatometry and gravimetry were in good agreement with each other (Supporting Information).

Before polymerization starts, the systems consist of monomer dissolved in the aqueous phase and inside the swollen monomer micelles (in the case of MMA and EMA monomers giving microemulsions) and inside monomer droplets (in the case of BMA, HMA, and 2-EHMA monomers giving emulsions). When polymerization is initiated, some of the swollen monomer micelles become particles by capturing radicals propagating in the aqueous phase (micellar nucleation). Particle formation can also occur by homogeneous nucleation when radicals in the aqueous phase grow until a critical size is reached, precipitating from the aqueous phase; these precipitated radicals can absorb surfactant and self-stabilize, giving a stable polymer particle as a result. In this article, high reaction rates (R_p) were observed in all polymerizations. Figure 1 shows the effects of the alkyl ester group of each monomer on the kinetics of microemulsion homopolymerization at two monomer contents (2.5 and 3.5%). Different marks represent the experimental data, while the continuous curves are predictions using the model reported by Morgan et al.³:

$$x = 1 \exp(-1/2\beta t^2) \quad (4)$$

where t is the time of reaction and β is given by the following expression:

$$\beta = \frac{2K_d K_p C_0 [I]}{M_0} \quad (5)$$

In eq. (5), $K_d = 1.86 \times 10^{-4} \text{ min}^{-1}$ and $[I] = 1.01 \times 10^{-3} \text{ mol/L}$, represent the dissociation constant and the initiator concentration, respectively. K_p is the propagation constant of monomer. C_0 and M_0 are the initial monomer concentration inside the particles and the initial macroscopic concentration of monomer in the reaction mixture in mol/L, respectively.

It can be seen from Figure 1 that for runs with 2.5% of monomer concentration, at 4 min of reaction, conversions higher

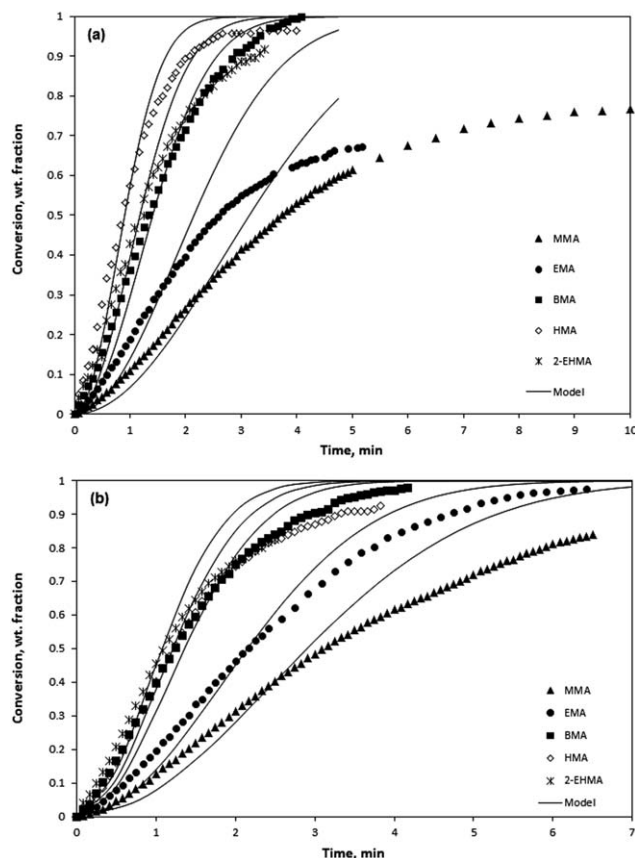


Figure 1. Conversion fractions vs. time for the different methacrylates homopolymerized in microemulsions at two different monomer concentrations. (a) 2.5% and (b) 3.5%. Symbols are experimental data obtained by dilatometry and the continuous curves are model predictions.

than 90% were obtained for BMA, HMA, and 2-EHMA, whereas only 63 and 53% conversion for EMA and MMA were observed. For 3.5% monomer concentration, conversions higher than 90% were observed for BMA, HMA, and 2-EHMA after 4 min of reaction, and only 85 and 61% conversions were observed for EMA and MMA, respectively. This behavior can be ascribed to the higher water solubility of EMA and MMA.

Figure 2 shows the polymerization rates obtained from the derivative of the experimental smoothed conversion data obtained by dilatometry. For 2.5 wt % of monomer concentration [Figure 2(a)], the order of polymerization rate was $R_{p,HMA} > R_{p,BMA} > R_{p,2-EHMA} > R_{p,EMA} > R_{p,MMA}$, whereas for 3.5 wt % of monomer concentration, the order of polymerization rate was $R_{p,BMA} > R_{p,HMA} > R_{p,2-EHMA} > R_{p,EMA} > R_{p,MMA}$ [Figure 2(b)]. Two periods of polymerization rate were observed, which is typical in microemulsion polymerization.

From Figure 1, it can be observed a deviation of the model from experimental data; therefore, the modeling of a complex reaction system with a single lumped parameter (the β values) is not reliable. This behavior is because of the model used here is a limiting case in which it was assumed that: (1) there is no bimolecular termination, neither in the aqueous phase nor in the particles, (2) capture of aqueous free radicals is fast (the

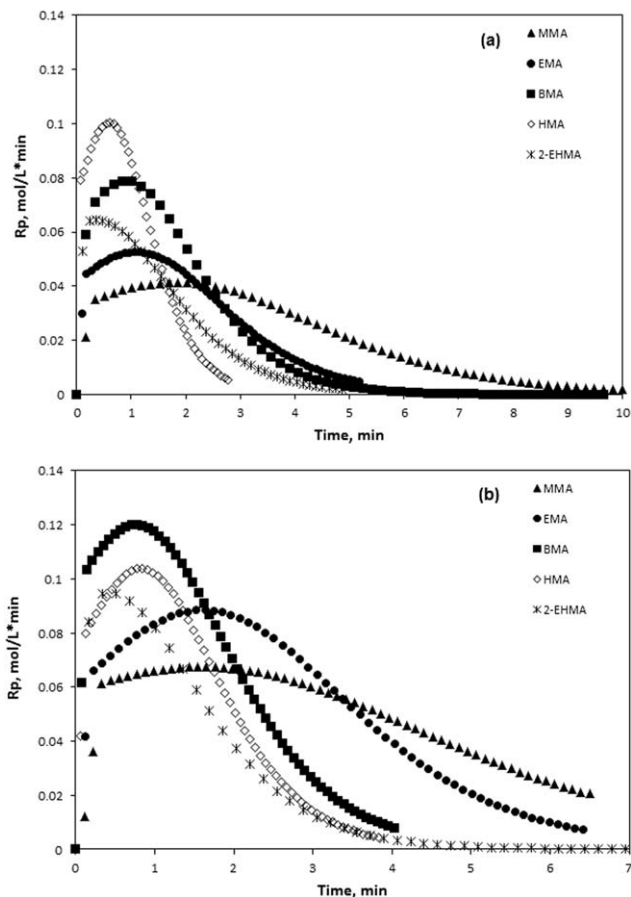


Figure 2. Polymerization rates as a function of time for the different methacrylates homopolymerized in microemulsions at two different monomer concentrations. (a) 2.5% and (b) 3.5%.

pseudo-first-order rate coefficient for capture of aqueous free radicals by micelles or particles is large and hence the concentration of radicals in the aqueous phase is negligible). Consequently, all radicals generated in the aqueous phase, either that obtained from initiator decomposition or those that exit from particles, are passed immediately to a swollen monomer micelle or to a dead particle, resulting in an active particle, and (3) the monomer concentration at the polymerization loci (generated active polymer particles) is proportional to the value of unity minus conversion x . The assumption implies that all unreacted monomer molecules reside homogeneously with generated polymer. These assumptions justify the assumption that the radical entry into growing particles is negligible compared to entry into swollen monomer micelles or dead particles, so that bimolecular termination in the particles can be neglected. As reported by Morgan et al.,³ this model fits well the experimental data for HMA. From eq. (5), it can be observed that β value for a particular monomer is a direct function of the C_0/M_0 ratio (mol fraction of monomer into the polymer particles with respect to the total monomer in the system); then, the slight independence of the β values with the monomer concentration for the hydrophobic monomers, can be due to the fact that monomer partitioning between the aqueous and organic phases in the system is negligible for hydrophobic monomers. However, the deviation

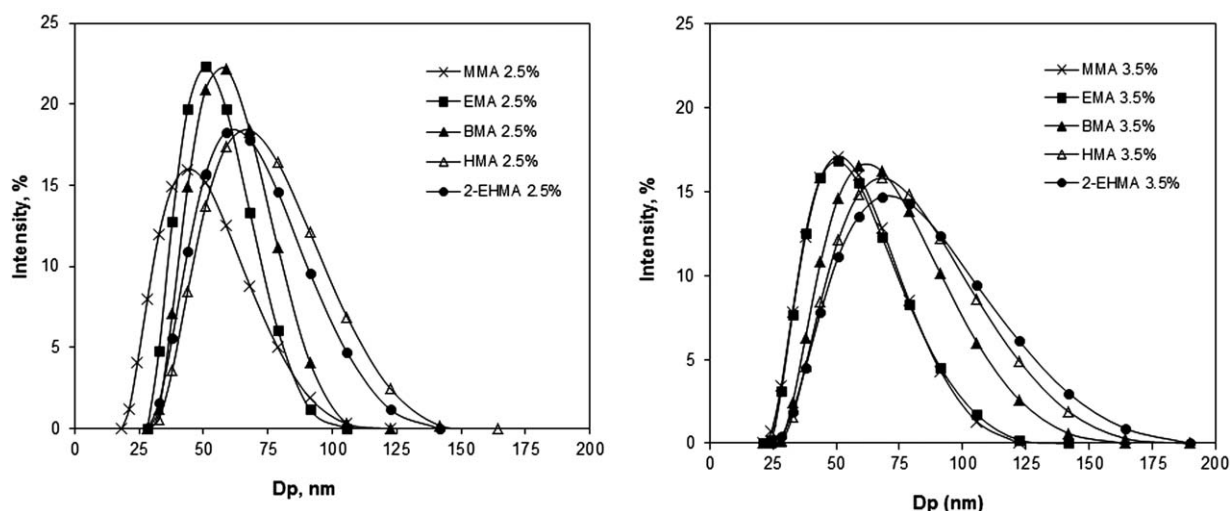


Figure 3. Particle size distribution of final latices obtained for the different runs and different monomer concentrations.

of the model from experimental data can be attributed not only to the monomer partitioning but also to other factors, such as different chain termination mechanisms (transfer reactions to monomer and to polymer), competing particle formation mechanisms (homogeneous and micellar nucleation), etc.

The number of particles (N_p) was calculated using eq. (6):

$$N_p = \frac{6M_0X}{\pi D_p^3 \rho_p} \quad (6)$$

where N_p is the number density of particles, $[M]_0$ is the initial monomer concentration in the reactor, X is the conversion, D_p is the experimental average diameter of the particles (with the assumption that they are spherical and mono-disperse) and ρ_p is the density of the polymer.

Table I shows D_p and N_p of the final latices obtained from polymerization of the different methacrylates at two monomer concentrations (2.5 and 3.5%). It can be observed that, D_p values are in the range of 42–65 nm. These values increased with the monomer concentration (more monomer solubilized with the same surfactant amount) and the hydrophobicity of mono-

mers, because swelling of the micelles increases (less monomer in the aqueous phase). Figure 3 shows the corresponding (PSDs). Narrower PSD were obtained for the hydrophilic monomers than for the hydrophobic monomers. Also, it can be observed from Table I that N_p decreases with the length of the alkyl ester group of monomers and increases with the monomer concentration. These results confirm that homogeneous nucleation predominates in the polymerization of hydrophilic monomers. In order to compare N_p with the kinetic behavior, the polymerization rates per particle (R_{pp}) were calculated as R_p/N_p (Table I). R_{pp} values can be taken as a semi-quantitative equivalent of the average number of radicals per particle.¹² Therefore, for both monomer concentrations studied, the number of radicals per particle increased with the length of the alkyl ester group of methacrylates, except for 2-EHMA. This is a consequence of the monomer hydrophobicity (less radical desorption from polymer particles), giving bigger particle diameters as a result and also the propagation rate constants for the monomers used are not so different from each other.

Table II shows the weight average molecular weight (M_w) and polydispersity (PDI) of polymers obtained from homopolymerization of the different methacrylates with 2.5% of monomer concentration. Values of M_w were in the range of 453,200–

Table I. Average Particle Diameters (D_p) and Number of Particles (N_p) of Final Latices Using Different Concentrations of Alkyl Ester Methacrylates

Monomer	D_p (nm)		$N_p \times 10^{-17}$ (#/L)		$R_{pp} \times 10^{-15}$ [mol/(min*particle)]	
	2.50%	3.50%	2.50%	3.50%	2.50%	3.50%
MMA	42	46	4.7	5.4	0.88	1.24
EMA	50	54	3.1	4.1	2.04	2.14
BMA	56	60	2.8	3.2	2.80	3.74
HMA	64	65	1.9	2.6	5.20	4.27
2-EHMA	59	64	2.6	2.9	4.50	3.76

R_{pp} = polymerization rate (maximum) per particle.

Table II. Weight Average Molecular Weight and Polydispersity Index of Polymers Obtained From Homopolymerization of Different Methacrylates with 2.5% of Monomer Concentration

Monomer	M_w (g/mol)	PDI ^a
MMA	453200	2.85
EMA	847000	3.05
BMA	1173000	1.83
HMA	2784000	1.65
2-EHMA	1928000	2.21

^aPDI = M_w/M_n .

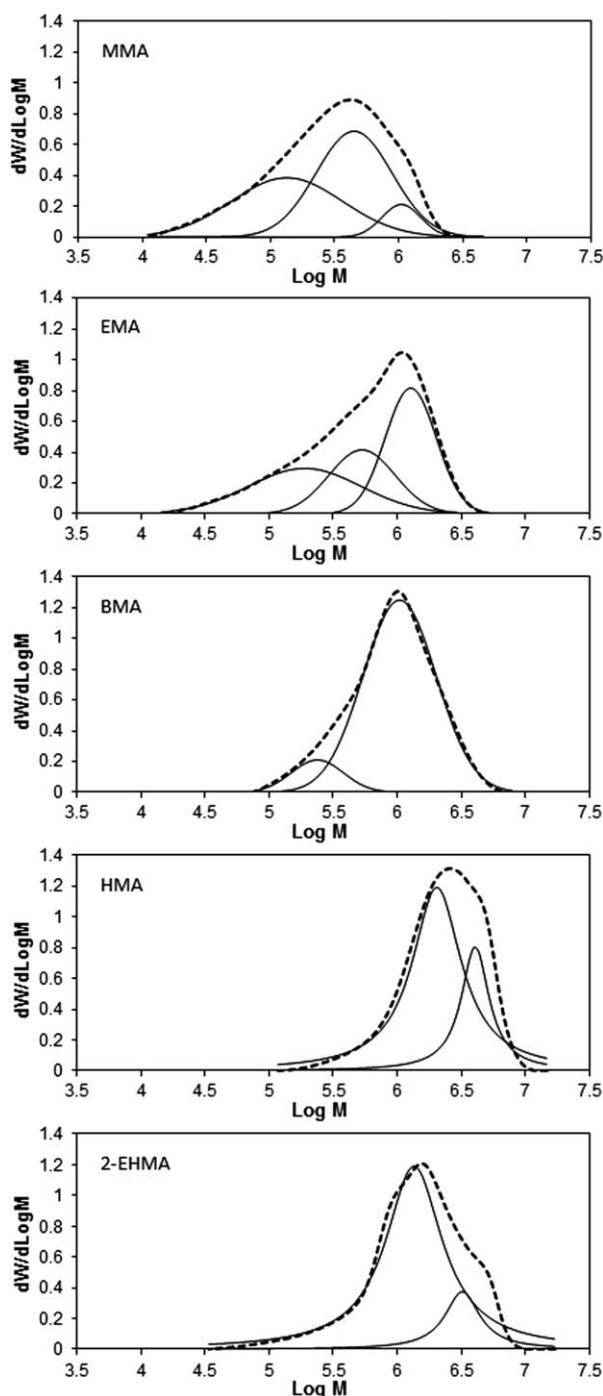


Figure 4. Molar masses distributions (MWD) of the polymers at the end of reaction for 2.5% of monomer concentrations. Dotted curves are experimental data and the continuous curves are deconvolutions using Gaussian's fits.

2,784,000 g/mol increasing with the hydrophobicity of the monomers. PDI values were between 1.6 and 3.0, which indicates that more than one chain termination mechanism occurs. Figure 4 shows the experimental molecular weight distributions (MWD) data (dotted curves) of the polymers at the end of polymerization and the corresponding deconvolutions using Gaussian fits (continuous curves). The MWD are relatively

narrow in all cases with three populations for the MMA and EMA. Concerning to BMA, HMA, and 2-EHMA, only two populations can be observed. In batch heterophase polymerization bimolecular termination is almost absent because of the compartmentalization effect. Consequently, M_w is high because transfer to monomer is the dominant mechanism for termination of chains' growth.¹⁴ The first population corresponding to low molecular weights can be related with bimolecular termination in the aqueous phase (which agrees with the hydrophilicity of MMA and EMA). The second population is due to chain transfer to monomer or bi-molecular termination (due to the 0–1 kinetics), and finally the third population, corresponding to high molecular weights, is usually observed when events as chain transfer to polymer are present. This behavior observed here is associated with the particles' sizes. That is, the smaller the D_p , the higher the bi-molecular termination, because when a growing particle captures a radical from the aqueous phase, the particle becomes inactive. Nevertheless, for higher D_p values, a radical entering to a growing particle can start a new polymer chain instead of the generation of an inactive particle, giving as a result higher M_w .

T_g is a valuable characterization parameter associated with the material properties and can provide very useful information regarding the end-use performance of a product. In general, factors increasing the stiffness of the polymeric molecular segments will tend to increase T_g .¹⁵ Moreover, T_g is commonly related to the stereochemistry of polymer chains (tacticity) as well as the molecular weight (T_g increases proportionally with the molecular weight). A semicrystalline polymer is composed of two main phases: amorphous and crystalline. In general, the T_g value will increase somewhat as the crystalline phase of the polymer increases. As explained by Tang et al.,⁴ the rich-syndiotacticity of the resulting polymers may be caused by the effect of volume restriction in nanoparticles. It is considered that in a confined volume of a latex particle formed in microemulsion, the propagating polymer chains must be organized in a gauche conformation than in its unperturbed state (mainly near the surface of the particle), the path of its random walk would be forced to fold back into the particle. For a polymer with final T_g above of the reaction temperature, at the beginning of chain propagation, the propagating chains have low molecular weights and low T_g values, accordingly, therefore, the restricted volume effect is relatively not so obvious at this stage. As the molecular weights and T_g s of the propagating chains increase, the T_g s exceed the reaction temperature, and then propagating chains pass a glass transition process and their free walks are more restricted. So the restricted volume effect became obvious, resulting in products with high syndiotacticities and higher glass transition temperatures.

Tacticity properties of the different polymethacrylates were evaluated by ¹³C-NMR spectroscopy. All spectra were analyzed in two signal regions: one that covers the signals corresponding to the carbonyl groups between 180 and 175 ppm (Figure 5) and the second that corresponds to signals belonging to the quaternary carbon between 46 and 43 ppm (Figure 6). The areas under the curves of the different signals in each region were calculated according to the signals to ¹³C attributed to mm

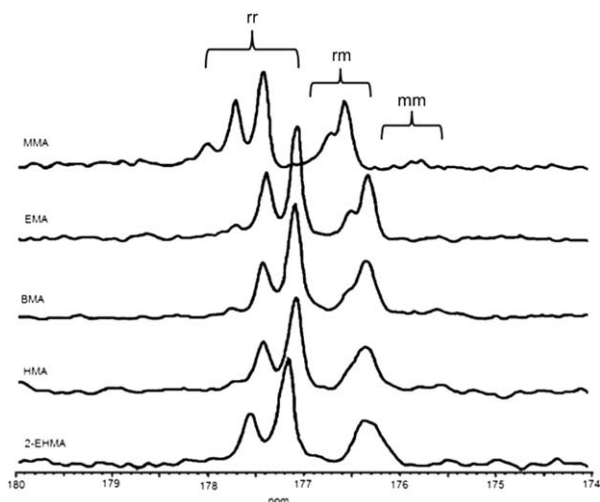


Figure 5. ^{13}C -NMR spectra in the zone of the carbonyl group showing the signals corresponding to rr, rm, and mm triads (syndiotactic, atactic, and isotactic, respectively) of methacrylate polymers synthesized with 3.5% of monomer concentrations.

(isotactic), rm (atactic), and rr (syndiotactic) triads.^{16,17} From the carbonyl and quaternary carbon regions (Figures 5 and 6, respectively) the signals of the three possible polymer configurations (mm, mr, and rr) are observed. Furthermore, the highest signal intensity (area) in both spectra is denoted for syndiotactic (rr) configuration in all polymers. The area of rr signals was used to calculate the syndiotacticity percentage by means of eq. (3). Table III shows the percentage values and their average of syndiotacticity of each polymer calculated from the two regions of ^{13}C -NMR spectra. In the same Table III are listed the T_g values calculated from DSC analysis (shown in Figure 7) for the different homopolymers studied. From Table III it is possible to observe that syndiotacticity values calculated from the carbonyl and quaternary carbon groups were similar and also increased with the length and steric effect of the alkyl pendant group in the polymer chain, while T_g values decrease, as can be also seen

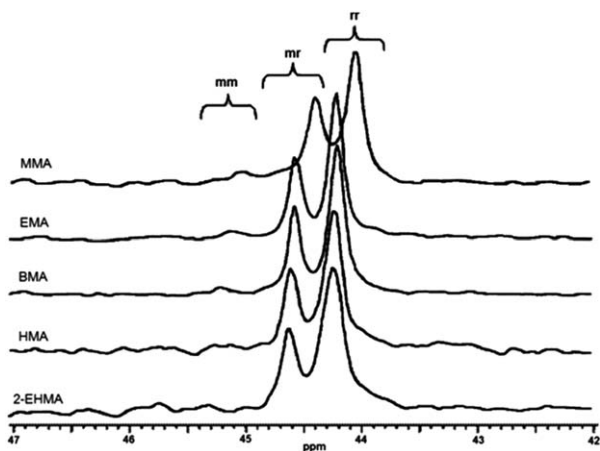


Figure 6. ^{13}C -NMR spectra in the zone of the quaternary carbon showing the signals corresponding to rr, rm, and mm triads (syndiotactic, atactic, and isotactic, respectively) of methacrylate polymers synthesized with 3.5% of monomer concentrations.

Table III. Syndiotacticity and T_g Values of Polymers Determined from the Areas Corresponding to Carbonyl and Quaternary Carbon Signals of Samples with 3.5% of Monomer Concentration

Monomer	Carbonyl C=O (%)	Quaternary carbon (%)	Average ^a (%)	T_g ($^{\circ}\text{C}$)
MMA	81	79	80.0	120
EMA	83	83	83.0	71
BMA	82	83	82.5	30
HMA	84	85	84.5	3
2-EHMA	87	87	87.0	-7

^a Calculated as the simple arithmetic average of values obtained from the carbonyl group and the quaternary carbon.

from Figure 7. Changes in the slopes of the heat flow curves are less noticeable by increasing the length of the alkyl group of the polymethacrylates.

The T_g and syndiotacticity exhibited by a polymer is dependent upon the synthetic route of the material. For example, Tang et al.⁷ reported the polymerizations of MMA, EMA, CHMA, iBMA, and BzMA in a seeded semicontinuous regime, finding syndiotacticities between 51 and 72%, decreasing with the reaction temperature. The D_p values of the corresponding latices were in the range of 13–31 nm. In our case, polymerizing in batch mode, high syndiotacticity percentages were obtained (80–87%) and latices with D_p between 42 and 65 nm. This difference in syndiotacticities is explained as follows: in a batch polymerization, the system is monomer flooded, giving as a result bigger particles' sizes than those obtained in a semicontinuous regime, in which polymeric nanoparticles growth is controlled with the monomer addition rate resulting in smaller D_p values. As previously discussed, bigger D_p gives higher molecular weights because of chain transfer to monomer events are accompanied with chain transfer to polymer and because bimolecular termination by capturing a second radical from the aqueous phase is less frequent; then, for higher molecular weights, steric hindrance forces the polymer chain to acquire syndiotactic configurations, preferentially.

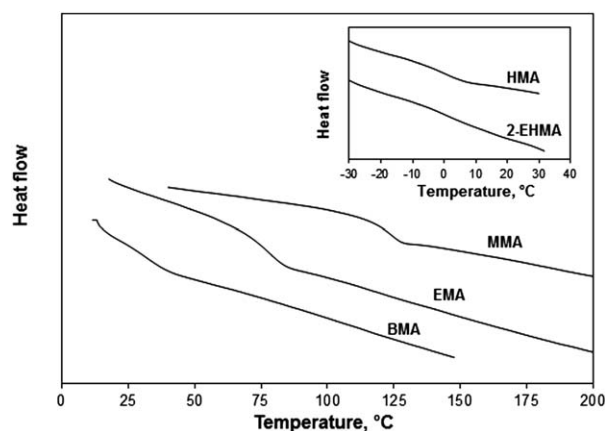


Figure 7. Heat flow versus temperature obtained from DSC analysis of the polymers at the end of reaction for 2.5% of monomer concentrations used.

CONCLUSIONS

MMA, EMA, BMA, HMA, and 2-EHMA were homopolymerized in heterophase systems in a batch mode. The kinetics study revealed that for 2.5 wt % of monomer concentration, the order of polymerization rate was $R_{p\text{HMA}} > R_{p\text{BMA}} > R_{p2\text{-EHMA}} > R_{p\text{EMA}} > R_{p\text{MMA}}$, whereas for 3.5 wt % of monomer concentration, the order of polymerization rate was $R_{p\text{BMA}} > R_{p\text{HMA}} > R_{p2\text{-EHMA}} > R_{p\text{EMA}} > R_{p\text{MMA}}$. The mathematical model used to represent the kinetics was not able to represent experimental kinetic data, which was ascribed not only to the monomer partitioning between the phases but also to factors, such as different chain termination mechanisms (transfer to monomer and to polymer) and particle formation mechanisms (homogeneous and micellar nucleation).

Dp values were in the range of 42–65 nm, increasing with the monomer concentration and the hydrophobicity of monomers. Values of Mw were in the interval of 453,200–2,784,000 g/mol increasing also with the hydrophobicity of the monomers. The PDI were high, ranging between 1.6 and 3.0, which can indicate more than one chain termination mechanism. Polymers with very high syndiotacticities were obtained (80–87%) because the higher molecular weights from batch mode polymerization (compared with the previously reported in the literature for seeded semicontinuous regime) forces the polymer chain to acquire syndiotactic configurations preferentially as a result of the higher steric hindrance.

ACKNOWLEDGMENTS

This work was supported by the Consejo Nacional de Ciencia y Tecnología, México (Grant # SEP-80843). Author V.M.O.M. acknowledges to Camerina J. Guzman-Alvarez for her help in polymer samples purifications.

REFERENCES

1. Antonietti, M.; Tauer, K. *Macromol. Chem. Phys.* **2003**, *204*, 207.
2. Martínez-Gutiérrez, H.; Ovando-Medina, V. M.; Peralta, R. D.; Mendizábal, E.; Puig, J. E. *Polym Eng Sci* **2013**, *53*, 1990.
3. Morgan, J. D.; Lusvardi, K. M.; Kaler, E. W. *Macromolecules* **1997**, *30*, 1897.
4. Tang, R.; Yang, W.; Zha, L.; Fu, S. *J. Macromol. Sci. Pure Appl. Chem.* **2008**, *45*, 345.
5. Kaler, E. W.; Hermanson, K. D. *Macromolecules* **2003**, *36*, 1836.
6. Kaler, E. W.; Hermanson, K. D. *J. Polym. Sci. Part A: Polym. Chem.* **2004**, *42*, 5253.
7. Katime, I.; Arellano, J.; Mendizábal, E.; Puig, J. E. *Eur. Polym. J.* **2001**, *37*, 2273.
8. Kaler, E. W.; Co, C.C.; de Vries, R. *Macromolecules* **2001**, *34*, 3224.
9. Kaler, E. W. de Vries, R.; Co, C.C. *Macromolecules* **2001**, *34*, 3233.
10. Mendizábal, E.; Flores, J.; Corona, M. A.; Moscoso, F. J.; Oseguera, O.; Manríquez, R.; López-Dellamary, F. A. *Rev Mex Ingeniería Química* **2011**, *10*, 125.
11. Katime, I.; Arellano, J.; Mendizábal, E.; Puig, J. E. *Eur. Polym. J.* **2001**, *37*, 2273.
12. Frisch, H.; Mallows, C.L.; Bovey, F.A. *J. Chem. Phys.* **1966**, *45*, 1565.
13. Capek, I.; Juranicova, V. *J. Polym. Sci. Part A: Polym. Chem.* **1996**, *34*, 575.
14. Ovando-Medina, V. M.; Peralta, R. D.; Mendizábal, E. *Colloid Polym. Sci.* **2009**, *287*, 561.
15. Sichina, W.J. Measurement of Tg by DSC. Thermal Analysis: Application Note. Perkin Elmer ZDA: Norwalk, CT, 2000.
16. Ferguson, R. C.; Ovenall, D. W. *Macromolecules* **1987**, *20*, 1245.
17. Brar, A. S.; Singh, G.; Shankar, R. J. *Mol. Struct.* **2004**, *703*, 69.